

RESEARCH ACTIVITIES IV

Department of Molecular Assemblies

IV-A Spectroscopic Study of Organic Conductors

The reflectivity of an organic conductor provides us with a wealth of information on the electronic structure. For instance, the anisotropy of a band structure, bandwidth, effect of electron-electron correlation, and electron-molecular vibration (EMV) coupling parameters can be extracted from the analysis of the reflectivity or optical conductivity curve. We are investigating the polarized reflection spectra of various organic conductors in the spectral region of 50–33000 cm^{-1} and in the temperature range of 6–300 K. Raman spectroscopy is a complementary method to reflection spectroscopy for understanding molecular vibrations (local phonons). We are investigating the charge ordering (CO) or charge disproportionation phenomena in organic conductors using the technique of vibrational spectroscopy. The charge ordering was found in inorganic narrow-band systems such as copper, manganese, and vanadium oxides. Recently, a charge-ordered ground state has been found in several organic conductors. The Raman and infrared spectra change dramatically at CO phase-transition temperature. Our goal is the complete understanding of the CO phase transition through the interpretation of the vibrational spectra, and the drawing of a P-T phase diagram using Raman spectra.

IV-A-1 Charge Ordering in θ -(BEDT-TTF)₂RbZn(SCN)₄ Studied by Vibrational Spectroscopy

YAMAMOTO, Kaoru; YAKUSHI, Kyuya;
MIYAGAWA, Kazuya¹; KANODA, Kazushi¹;
KAWAMOTO, Atsushi²
(¹Univ. Tokyo; ²Hokkaido Univ.)

[Phys. Rev. B submitted]

Spatial charge distribution in an insulating phase of θ -(BEDT-TTF)₂RbZn(SCN)₄ was investigated using polarized Raman and infrared (IR) spectroscopy. Figure 1 shows polarized Raman and IR spectra of the natural (non-substituted) and ¹³C-substituted samples in the insulating phase. Both the Raman and IR spectra showed a complicated multiple-peak pattern stemming from two modes based on ring (ν_2) and central C=C stretchings (ν_3). From the isotope-shifts, we attributed peaks **a**₁ and **a**₂ to ν_2 and peaks **b**₁, **b**₂, **c**₁, and **c**₂ to ν_3 . While it is known that ν_2 and ν_3 commonly show a large frequency shift in proportion to a variation in the molecular charge, ν_3 provides a larger vibronic coupling effect than ν_2 . Because of the strong vibronic-coupling, ν_3 -related peaks showed a large Davydov splitting, allowing us to perform factor group analysis to specify the spatial pattern of the charge distribution. Meanwhile, the strong vibronic coupling causes an irregular frequency shift, hindering us to calculate the charge-disproportionation (CD) ratio from the frequency. To avoid the complicated shift due to the vibronic coupling, we used the weakly coupled mode ν_2 for the estimation of the CD ratio. The calculated ratio agrees with the value estimated by an NMR study. The agreement of the conclusions drawn by the two different approaches substantiates the explanation for the charge distribution and the reliability of this estimation method.

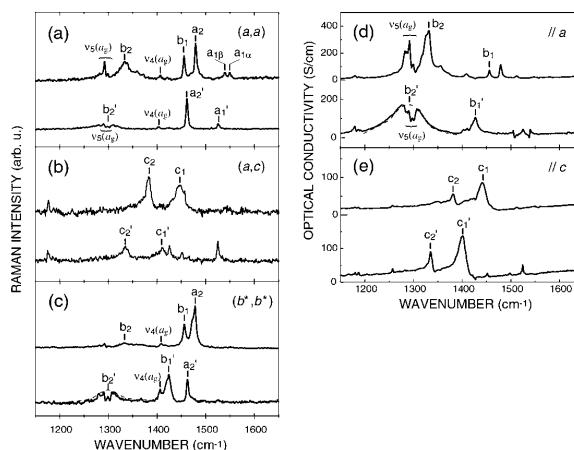


Figure 1. Polarized Raman and optical conductivity spectra of the natural (upper curve) and ¹³C-substituted (lower curve) θ -(BEDT-TTF)₂RbZn(SCN)₄. (a), (b), and (c) show the (a,a), (a,c), and (b*,b*)-polarized Raman spectra, and (d) and (e) show the a- and c-polarized optical conductivity spectra, respectively. ($T = 50$ K)

IV-A-2 Charge Disproportionation Ratio of (BEDT-TTF)₃CuBr₄ Studied by a Molecular Vibration Frequency

YAMAMOTO, Kaoru; YAKUSHI, Kyuya;
YAMAURA, Jun-ichi¹; ENOKI, Toshiaki²
(¹Inst. Solid State Phys.; ²Tokyo Inst. Tech.)

Vibrational spectroscopy is a powerful tool to investigate charge distribution in charge transfer salts. Based on Raman and IR measurements for θ -(ET)₂RbZn(SCN)₄, (ET: BEDT-TTF) we have proposed that a molecular charge can be estimated from the frequency of the ring C=C stretching mode (ν_2). In order to verify the reliability of the argument, we applied this analysis to other ET salts with a different molecular arrangement and band filling from the θ -type salt. The title compound (ET)₃CuBr₄ has a 3:1 stoichiometry. According to the x-ray diffraction study, the semi-

conductive salt shows charge ordering from room temperature. Raman spectra of this salt showed multiple peaks in the C=C stretching region. Based on the polarization dependence, we found two ν_2 -related peaks among the multiple peaks. Figure 1 shows the reported ν_2 frequencies plotted with respect to the molecular charge. According to this plot, the observed two peaks are positioned approximately at $+0.9e$ and $+0.2e$. Supposing that there are two differently charged ET molecules ($+0.9e$ and $+0.2e$) in the ratio of 2:1, the average molecular charge is consistent with the stoichiometry. This suggests the certainty of the interpretation. This result supports the conclusion of the x-ray study proposing the presence of charge ordering, and demonstrates that the molecular-charge-estimation based on the ν_2 frequency can be applied for various systems.

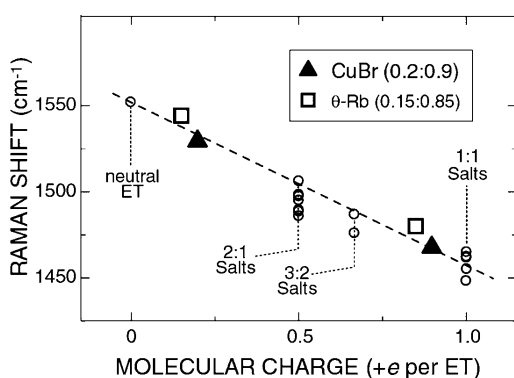
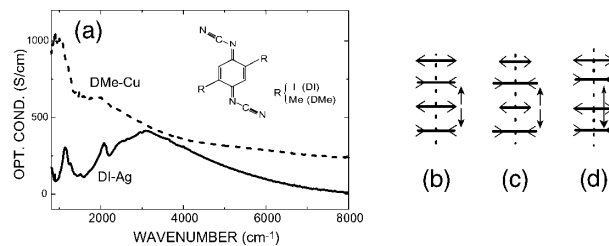


Figure 1. Raman frequencies of the ring C=C stretching (ν_2) modes vs. molecular charge.

IV-A-3 Charge and Molecular Arrangement in (DI-DCNQI)₂Ag Studied by Vibrational Spectroscopy

YAMAMOTO, Kaoru; YAKUSHI, Kyuya; HIRAKI, Koichi¹; TAKAHASHI, Toshihiro¹; KANODA, Kazushi²; MENEGHETTI, Moreno³
(¹Gakushuin Univ.; ²Univ. Tokyo; ³Univ. Padova, Italy)

(DI-DCNQI)₂Ag (see the inset of Figure 1) has a one-dimensional (1D) structure with a quarter-filled band. An x-ray diffraction and NMR studies revealed that there was a $4k_F$ charge-density wave (CDW) below 220 K. Both studies claim the $4k_F$ site CDW (see Figure 1c) for the insulating state of this compound. To examine the possible $4k_F$ bond CDW (see Figure 1d), we studied the molecular vibrations, since the vibronic modes are extremely sensitive to the lattice modulation such as bond CDW. As shown in Figure 1a, the optical conductivity spectrum of (DI-DCNQI)₂Ag shows clear vibronic bands below 3000 cm^{-1} , in contrast to (DMe-DCNQI)₂Cu, which is metallic with a uniform stacking structure. Because the CT dipole moments induced by EMV coupling are cancelled out in a uniform stack (1b) and $4k_F$ site CDW (1c) as shown in Figure 1, the appearance of the vibronic bands strongly suggests the $4k_F$ bond CDW (1d). Low-temperature Raman and IR measurements are in progress to examine whether the



bond CDW and site CDW coexist or not.

Figure 1. (a) Optical conductivity spectra of (DI-DCNQI)₂Ag (solid line) and (DMe-DCNQI)₂Cu (dashed line) measured at room temperature. Schematic models of vibronically induced charge-transfer moment in (a) uniformly stacked, (b) $4k_F$ site CDW, and (c) $4k_F$ bond CDW. Horizontal bars and arrows represent a charge density and phase of a molecular vibration, respectively. Perpendicular arrows indicate the CT dipole moments induced by the molecular vibration.

IV-A-4 The C=C Stretching Vibrations of κ -(BEDT-TTF)₂Cu[N(CN)₂]Br and Its Isotope Analogues

MAKSIMUK, Mikhail¹; YAKUSHI, Kyuya; TANIGUCHI, Hiromi²; KANODA, Kazushi²; KAWAMOTO, Atsushi³
(¹IMS and Inst. Problem Chem. Phys.; ²Tokyo Univ.; ³Hokkaido Univ.)

[J. Phys. Soc. Jpn. submitted]

The C=C stretching modes in resonance Raman spectra and infrared reflectivity were measured at temperatures between 15 K and 300 K using various polarizations in κ -(BEDT-TTF)₂Cu[N(CN)₂]Br, its fully and partially deuterated analogues. The infrared- and Raman-active bands were re-assigned based on the factor group analysis. As shown in Figure 1, we found a Raman-active EMV-coupled ν_3 mode near 1420 cm^{-1} , which has B_{2g} symmetry and shows a large downshift and broadening through the inter-dimer EMV interaction. The ν_2 and ν_3 modes are respectively the ring and bridge C=C stretching vibration, which mix with each other depending upon the positive charge on BEDT-TTF. We found that the mixing of the bridge and ring C=C stretching vibrations depended upon the symmetry of the crystal mode. The ν_{27} mode is an asymmetric ring C=C vibration, which vibrates out-of-phase within a dimer in the ν_{27} (A_g) crystal mode. In contrast to deuterated crystals, the non-deuterated crystals show a splitting in the ν_2 , ν_3 , and ν_{27} . The origin of this unusual finding is not clear at present.

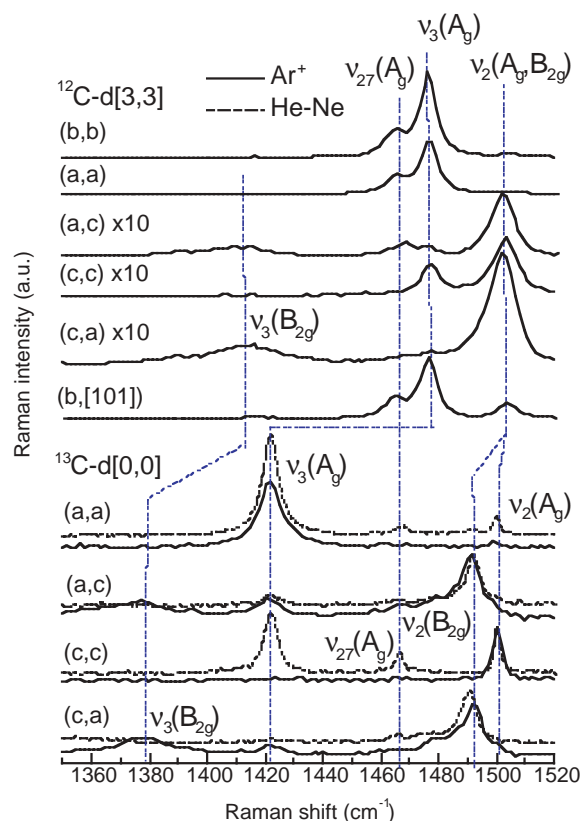


Figure 1. Raman spectra of $^{12}\text{C-d}[3,3]$ and $^{13}\text{C-d}[0,0]$ at 20 K. The intensity among the different polarizations is approximately scaled to each other in $^{12}\text{C-d}[3,3]$, but not scaled in $^{13}\text{C-d}[0,0]$. In $^{12}\text{C-d}[3,3]$, three hydrogen atoms in each ethylene group are replaced by deuterium, and in $^{13}\text{C-d}[0,0]$, the two central ^{12}C atoms bridging the 1,3-dithiol rings are replaced by the carbon isotope ^{13}C .

IV-A-5 Plasma Frequency and Optical Effective Mass of $\kappa\text{-(ET-d}_8)_2\text{Cu(CN)[N(CN)}_2]$

**DROZDOVA, Olga¹; YAKUSHI, Kyuya;
YAMOCHI, Hideki²; SAITO, Gunzi²**
(¹IMS and Yoffe Inst. Phys., ²Kyoto Univ.)

$\kappa\text{-(ET)}_2\text{Cu(CN)[N(CN)}_2]$ is a strongly correlated organic metal with superconducting transition at $T_C = 11.2$ K (ET-h₈) and $T_C = 12.3$ K (ET-d₈) at ambient pressure. Optical study was undertaken on single crystals of deuterated compound in a wide frequency region from far-IR to UV, along two main directions in the conducting (100) plane, at temperatures down to 6 K.

The tight-binding band calculation at 300 K predicts the intraband transition of the free charge carriers for two upper band branches, with the total calculated plasma frequency ~ 7000 cm^{-1} and the effective mass $m^*/m_e = 2$. However, in the experimental reflectivity spectra, the intraband transition appears at much lower frequency ($\omega < 300$ cm^{-1} at $T = 300$ K). Almost no Drude peak can be found in the optical conductivity, and most of the spectral weight is contained in the broad mid-infrared peak.

Two distinctive temperature regions can be found. From 300 K down to 150 K, intensity of the mid-

infrared peak increases together with the intensity of the coupled EMV features. Below 150 K, the far-infrared reflectivity starts to grow rapidly. In the optical conductivity, it is accompanied by the shift of the spectral weight from the mid-infrared peak and EMV coupled features to the Drude peak.

The parameters of the electronic structure (ω_p , Γ_e) were obtained from the Drude-Lorentz dispersion analysis. At lower temperatures, the plasma frequency is rapidly growing ($\omega_p \sim 5500$ cm^{-1} at 6 K). Ordinary sources of the low-temperature increase of the plasma frequency in a metal (Fermi-Dirac function, increase of the transfer integrals due to the crystal shrinking) cannot justify the observed three-to-four-fold growth. However, the growth of the plasma frequency can be explained by a temperature-dependent density of states in the strongly correlated metal accompanying a crossover from an incoherent transport at high temperatures to a coherent regime at lower T .

IV-A-6 Charge Order in $\theta\text{-(BDT-TTP)}_2\text{Cu(NCS)}_2$

**YAKUSHI, Kyuya; OUYANG, Jianyong¹;
SIMONYAN, Mkhitar²; MISAKI, Yohji³;
TANAKA, Kazuyoshi³**
(¹GUAS; ²IMS and Inst. Phys. Res. ARAS; ³Kyoto Univ.)

[*Mol. Cryst. Liq. Cryst.* in press]

$\theta\text{-(BDT-TTP)}_2\text{Cu(NCS)}_2$ is a highly correlated organic conductor with a quasi-two-dimensional electronic structure. We have found a charge disproportionation in $\theta\text{-(BDT-TTP)}_2\text{Cu(NCS)}_2$ accompanying the phase transition at 250 K.¹⁾ The magnetic properties of this compound was examined to know the pattern of the ordered charge. The paramagnetic susceptibility conforms to Curie-Weiss law down to about 30 K, makes a peak at 5–10 K, and drops to nearly zero at 1.8 K. This behavior suggests that the exchange interaction between localized charge is much weaker than that of $\theta\text{-(BEDT-TTF)}_2\text{RbZn(SCN)}_4$ which shows a similar charge ordering phase transition. This result and the comparison of the optical conductivity with a theoretical calculation strongly suggest that the localized charge forms a vertical stripe in contrast to the horizontal stripe in $\theta\text{-(BEDT-TTF)}_2\text{RbZn(SCN)}_4$. The horizontal stripe is more stable than the vertical stripe according to the calculation of Madelung energy in both compounds. The degree of charge disproportionation $\delta = 0.1\text{--}0.2$, in $(\text{BDT-TTP})^{\delta+}(\text{BDT-TTP})^{(1-\delta)+}$ is also almost the same as that of $\theta\text{-(BEDT-TTF)}_2\text{RbZn(SCN)}_4$ ($\delta = 0.15$). The investigation of the reasoning of the different nature between $\theta\text{-(BDT-TTP)}_2\text{Cu(NCS)}_2$ and $\theta\text{-(BEDT-TTF)}_2\text{RbZn(SCN)}_2$ is now in progress.

Reference

- 1) J. Ouyang, K. Yakushi, Y. Misaki and K. Tanaka, *Phys. Rev. B* **63**, 54301 (2001).

IV-A-7 Assignment of the In-Plane Molecular Vibrations of the Electron-Donor Molecule BDT-TTP Based on Polarized Raman and Infrared Spectra

**OUYANG, Jianyong¹; YAKUSHI, Kyuya;
KINOSHITA, Tomoko¹; NANBU, Shinkoh;
AOYAGI, Mutsumi; MISAKI, Yohji²; TANAKA,
Kazuyoshi²**
(¹GUAS; ²Kyoto Univ.)

[*Spectrochim. Acta, Part A* in press]

To interpret the change of the vibrational spectrum accompanying the charge ordering and/or asymmetric charge distribution within the BDT-TTP molecule, we conducted the normal mode analysis of BDT-TTP. We first analyzed TTP-DO which have a TTP skeleton in order to obtain the force constants in the TTP skeleton, and then analyzed BDT-TTP based on the empirical force constants. The vibrational modes of TTP-DO are assigned with the aid of the depolarization ratio of solution Raman spectra, polarized reflection and Raman spectra of single crystals. A D_{2h} symmetry is assumed for the BDT-TTP molecule and its in-plane fundamental vibrations are assigned with the aid of the polarization ratio and the correlation with TTP-DO, TTF, TMTTF, and BEDT-TTF. Normal coordinate calculation with a modified internal valence force field was carried out for the in-plane fundamental vibrations of TTP-DO and BDT-TTP. *Ab initio* calculations of the normal modes of BDT-TTP⁰ and BDT-TTP⁺ were compared with the empirical analysis. The agreement with the result of the empirical analysis was very good.

IV-A-8 Spectroscopic Study of the [0110] Charge Ordering in (EDO-TTF)₂PF₆

DROZDOVA, Olga¹; YAKUSHI, Kyuya; OTA, Akira²; YAMACHI, Hideki²; SAITO, Gunzi²
(¹IMS and Yoffe Inst. Phys.; ²Kyoto Univ.)

(EDO-TTF)₂PF₆ is a novel organic metal, which undergoes a complex phase transition at 280 K. The feature of the phase transition includes a sharp metal-insulator transition with 1st order canceling of the magnetic moment, order-disorder transformation of PF₆, drastic change in the donor packing and shape, and a charge ordering.

IR spectra at 295 K show the Drude-like reflectivity along the stack ($E||b$), and a low background with a number of phonons for the perpendicular ($E||a^*$) direction. The optical conductivity for $E||b$ displays a peak of $1500 \Omega^{-1}\text{cm}^{-1}$ centered at 1200 cm^{-1} , which extrapolates smoothly to the measured conductivity $\sigma_{dc} = 50 \Omega^{-1}\text{cm}^{-1}$. The peak has a distorted shape, with a dip due to the EMV coupling at 1400 cm^{-1} , and an extended high-frequency tail presumably due to the electron correlation effect. The electronic spectrum for $E||b$ changes drastically below the phase transition: the peak at 1200 cm^{-1} completely disappears, and instead two charge-transfer bands emerge. The first is of $D^0D^+ \rightarrow D^+D^0$ type, centered at 4500 cm^{-1} . It is the lowest electronic excitation of the low-temperature phase, and it compares well with the energy gap $E_g = 0.64 \text{ eV}$ measured on the compressed powder pellet. The second band is at 11150 cm^{-1} , corresponding to $D^+D^+ \rightarrow D^{2+}D^0$ charge transfer.

Profound change appears in the vibrational spectra

in the region of charge-sensitive C=C stretching modes, as well. Neutral EDO-TTF has three C=C modes: ν_1 (EDO-ring, 1648 cm^{-1}), ν_2 (TTF-ring, 1538 cm^{-1}), and ν_3 (central, 1498 cm^{-1}). In the high-temperature phase, three IR and three Raman active C=C modes are allowed and can be observed in the specific polarizations. Their frequencies correspond to EDO-TTF^{0,5+}. Below 280 K, these are split into a total of 12 modes (6 IR + 6 R), half due to the charge-poor EDO-TTF and half due to the charge-rich ones. ν_3 and ν_1 of the charge-rich EDO-TTF were found to be strongly interacting with the 11150 cm^{-1} charge-transfer band, as evidenced by both the IR spectrum along the stacking axis, and by the selective resonance Raman effect of these modes with the 785 nm excitation wavelength in the same direction. From the ionization shifts, it was estimated that the charge on the charge-poor and charge-rich molecules is $\leq +0.1e$ and $\geq +0.9e$, respectively, *i.e.* the charge is completely separated.

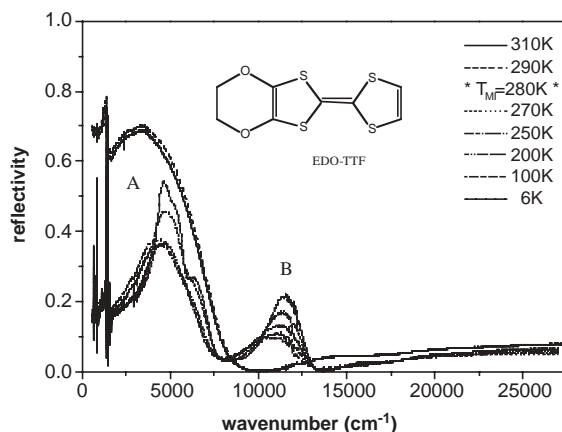


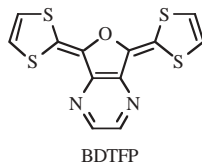
Figure 1. Temperature dependence of the reflection spectrum of EDO-TTF. The spectrum drastically changes from a metallic to insulating reflectivity at the phase transition temperature. The bands A and B correspond to the charge-transfer transitions of $D^+D^0 \rightarrow D^0D^+$ and $D^+D^+ \rightarrow D^0D^{2+}$, which clearly indicate the charge ordering such as $D^0D^+D^+D^0$.

IV-A-9 Structural and Spectroscopic Study of Quasi-One-Dimensional Organic Conductor, (BDTFP)₂X(C₆H₅Cl)_{0.5} (X = AsF₆, PF₆)

**URUICHI, Mikio; YAKUSHI, Kyuya;
SHIRAHATA, Takashi¹; TAKAHASHI, Kazuko¹;
MORI, Takehiko²; NAKAMURA, Toshikazu**
(¹Tohoku Univ.; ²Tokyo Inst. Tech.)

In (BDTFP)₂X(PhCl)_{0.5} (X = PF₆, AsF₆), the BDTFP molecules are stacked along the *c*-axis with a dimerized structure. The crystal structure and polarized reflection spectra suggest a quasi-1D electronic structure along the *c*-axis. In spite of the isomorphous structure at room temperature, the PF₆ and AsF₆ salts show different kinds of phase transition. (BDTFP)₂PF₆(PhCl)_{0.5} shows a magnetic phase transition at 175 K accompanying a resistivity jump, and undergoes a non-magnetic ground state. On the other hand, (BDTFP)₂AsF₆(PhCl)_{0.5} shows a first-order phase transition at 250 K, and undergoes first a paramagnetic state and then an anti-ferromagnetic ground state. We determined the low-temperature

crystal structures below the phase transition temperature. In the former, the *c*-axis was doubled and thus the dimerized structure changed into a tetramerized structure. At the same time, a new charge-transfer transition appeared at 7000~8000 cm^{-1} . These two findings are consistent with the non-magnetic state. In the latter, on the other hand, dimerized structure was maintained below the phase transition temperature, and instead AsF_6^- ion rotated with *ca.* 10° rotation of BDTFP. This structural change seems to be the origin of the first-order phase transition to a paramagnetic state.



References

- 1) T. Ise, T. Mori and K. Takahashi, *J. Mater. Chem.* **11**, 264 (2001).
- 2) T. Nakamura, K. Takahashi, T. Ise, T. Shirahata, M. Uruichi, K. Yakushi and T. Mori, *Mol. Cryst. Liq. Cryst.* in press.

IV-A-10 Crystal Chemistry and Physical Properties of Superconducting and Semiconducting Charge Transfer Salts of the Type $(\text{BEDT-TTF})_4[\text{A}^I\text{M}^{\text{III}}(\text{C}_2\text{O}_4)_3] \text{PhCN}$ ($\text{A}^I = \text{H}_3\text{O}^+, \text{NH}_4^+, \text{K}^+$; $\text{M}^{\text{III}} = \text{Cr}, \text{Fe}, \text{Co}, \text{Al}$; BEDT-TTF = Bis(ethylenedithio) tetrathiafulvalene)

MARTIN, Lee¹; TURNER, Scott T.¹; DAY, Peter¹; GUIONNEAU, Philippe²; HOWARD, Judith A. K.³; HIBBS, Dai E.⁴; LIGHT, Mark E.⁴; HURSTHOUSE, Michel B.⁴; URUICHI, Mikio; YAKUSHI, Kyuya
 (¹Royal Inst. GB; ²Inst. Chim. Matière Condensée de Bordeaux; ³Univ. Durham; ⁴Univ. Southampton)

[*Inorg. Chem.* **40**, 1363 (2001)]

Synthesis, structure determination by single-crystal X-ray diffraction, and physical properties are reported and compared for superconducting and semiconducting molecular charge-transfer salts with stoichiometry

$(\text{BEDT-TTF})_4[\text{A}^I\text{M}^{\text{III}}(\text{C}_2\text{O}_4)_3] \text{PhCN}$, where $\text{A}^I = \text{H}_3\text{O}^+, \text{NH}_4^+, \text{K}^+$; $\text{M}^{\text{III}} = \text{Cr}, \text{Fe}, \text{Co}, \text{Al}$. Attempts to substitute M^{III} with Ti, Ru, Rh, or Gd are also described. New compounds with $\text{M} = \text{Co}$ and Al are prepared and detailed structural comparisons are made across the whole series. Compounds with $\text{A} = \text{H}_3\text{O}^+$ and $\text{M} = \text{Cr}, \text{Fe}$ are monoclinic (space group $C2/c$), at 150, 120 K $a = 10.240(1) \text{ \AA}, 10.232(2) \text{ \AA}; b = 19.965(1) \text{ \AA}, 20.04(3) \text{ \AA}; c = 34.905(1) \text{ \AA}, 34.97(2) \text{ \AA}; \beta = 93.69(1)^\circ, 93.25(1)^\circ$, respectively, both with $Z = 4$. These salts are metallic at room temperature, becoming superconducting at 5.5(5) or 8.5(5) K, respectively. A polymorph with $\text{A} = \text{H}_3\text{O}^+$ and $\text{M} = \text{Cr}$ is orthorhombic ($Pbcn$) with $a = 10.371(1) \text{ \AA}, b = 19.518(3) \text{ \AA}, c = 35.646(3) \text{ \AA}$, and $Z = 4$ at 150 K. When $\text{A} = \text{NH}_4^+$, $\text{M} = \text{Fe}, \text{Co}, \text{Al}$, the compounds are also orthorhombic ($Pbcn$), with $a = 10.370(5) \text{ \AA}, 10.340(1) \text{ \AA}, 10.318(7) \text{ \AA}; b = 19.588(12) \text{ \AA}, 19.502(1) \text{ \AA}, 19.460(4) \text{ \AA}, c = 35.646(3) \text{ \AA}, 36.768(1) \text{ \AA}, 35.808(8) \text{ \AA}$ at 150 K, respectively, with $Z = 4$. All of the $Pbcn$ phases are semiconducting with activation energies between 0.15 and 0.22 eV. For those compounds which are thought to contain H_3O^+ , Raman spectroscopy or C=C and C-S bond lengths of the BEDT-TTF molecules confirm the presence of H_3O^+ rather than H_2O . In the monoclinic compounds the BEDT-TTF molecules adopt a β'' packing motif while in the orthorhombic phases $(\text{BEDT-TTF})_2$ dimers are surrounded by monomers. Raman spectra and bond length analysis for the latter confirm that each molecule of the dimer has a charge of +1 while the remaining donors are neutral. All of the compounds contain approximately hexagonal honeycomb layers of $[\text{AM}(\text{C}_2\text{O}_4)_3]$ and PhCN, with the solvent occupying a cavity bounded by $[\text{M}(\text{C}_2\text{O}_4)_3]^{3-}$ and A. In the monoclinic series each layer contains one enantiomeric conformation of the chiral $[\text{M}(\text{C}_2\text{O}_4)_3]^{3-}$ anions with alternate layers having opposite chirality, whereas in the orthorhombic series the enantiomers form chains within each layer. Analysis of the supramolecular organization at the interface between the cation and anion layers shows that this difference is responsible for the two different BEDT-TTF packing motifs, as a consequence of weak H-bonding interactions between the terminal ethylene groups in the donor and the $[\text{M}(\text{C}_2\text{O}_4)_3]^{3-}$ oxygen atoms.

IV-B Solid State Properties of Organic Conductors with π -d Interaction

Some phthalocyanine molecules contain unpaired d-electrons in the conjugated π -electron system. Due to this nature, the itinerant π -electrons coexist with localized unpaired d-electrons in solid phthalocyanine salts, in which a one-dimensional double-chain system (metal and ligand chain) is formed. Furthermore these chains make up wide (π -band) and narrow (d-band) one-dimensional bands. The energy of the narrow band is close to the Fermi energy of the wide band. The phthalocyanine conductor is thus a two-chain and two-band system. The electronic structure of phthalocyanine conductors is analogous to that of the f-electron system, in which a narrow f-band coexists with a wide s-band and they are hybridized near the Fermi level. To understand the electronic structure of this two-band system, we are investigating the charge-transfer salts of NiPc and CoPc and their mixed crystals.

IV-B-1 Preparation and Characterization of Phthalocyanine-Based Organic Alloy $\text{Co}_x\text{Ni}_{1-x}\text{Pc}(\text{AsF}_6)_{0.5}$ ($0 \leq x \leq 1$)

DING, Yuqin¹; SIMONYAN, Mkhitar²; YONEHARA, Yukako¹; URUICHI, Mikio; YAKUSHI, Kyuya

(¹GUAS; ²IMS and Inst. Phys. Res. ARAS)

[*J. Mater. Chem.* **11**, 1469 (2001)]

The organic alloy $\text{Co}_x\text{Ni}_{1-x}\text{Pc}(\text{AsF}_6)_{0.5}$ ($0 \leq x \leq 1$) was prepared and characterized by elementary analysis (EPMA), X-ray diffraction, ESR, magnetic susceptibility, Raman spectroscopy and reflection spectroscopy. These experiments show that mixed crystals are formed for a wide range of x although $\text{CoPc}(\text{AsF}_6)_{0.5}$ is not exactly isomorphous to $\text{NiPc}(\text{AsF}_6)_{0.5}$. The mixing on a molecular level is proved by the x dependence of the ESR and Raman spectra over the whole range of x . The localized spin on Co^{2+} occupies the $3d_{z^2}$ orbital, which is extended to the stacking axis. The reflection spectrum shows that this d orbital forms a one-dimensional band along the stacking axis and closely located near the Fermi level of $3/4$ -filled π band. We found a very weak $3d_{z^2}$ -to- $3d_{x^2-y^2}$ inter-molecular charge transfer transition through the resonance effect of Raman spectrum in the alloy system. Based on the above results, we proposed a model for the energy band near the Fermi level including the 3d bands. This band model explained the differences in the magnetic and optical properties between $\text{CoPc}(\text{AsF}_6)_{0.5}$ and $\text{NiPc}(\text{AsF}_6)_{0.5}$.

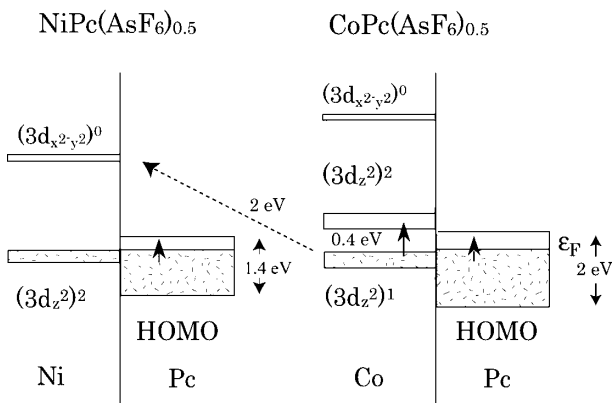


Figure 1. Schematic band structure including 3d bands. The arrows denote the optical transition along the conducting axis detected in the reflection spectra and through resonance effect of Raman spectrum.

IV-B-2 Electronic States and Infrared Spectroscopy of Nickel and Cobalt Phthalocyanines: *Ab initio* Calculations for the Neutral and Cation States

TOMAN, Petr¹; NESPUREK, Stanislav¹; YAKUSHI, Kyuya

(¹Inst. Macromolecular Chem. ASCR)

[*Synth. Met.* submitted]

Organic conductors such as TMTSF, BEDT-TTF,

and DCNQI have charge sensitive vibrational bands, which show red shift upon oxidation or reduction. This phenomenon comes from the reorganization of the molecular geometry. By contrast, metallophthalocyanine (MPc) has no such vibrational bands, because the molecular geometry is rigid against the oxidation. However, MPc has characteristic vibrational bands, the intensity of which changes upon oxidation. The reason for this change is associated with the change of the charge distribution between neutral and oxidized MPc. We calculated the frequency and intensity of the normal mode of NiPc and CoPc by the B3LYP method. This *ab initio* calculation clearly showed the ligand oxidation both in NiPc and CoPc, which agreed with the experimental observation. Besides, the calculation reproduced the frequency of the infrared-active modes, and the intensity changes of the characteristic bands: the 1291, 1356, 1471, and 1533 cm^{-1} bands of NiPc and 1290, 1468, and 1525 cm^{-1} bands of CoPc.

Using the molecular orbitals, the overlap integrals are calculated between a_{1u} HOMO a MPc and the a_{1g} $3d_{z^2}$ orbital of the adjacent molecule in $\text{MPc}(\text{AsF}_6)_{0.5}$. The extremely small overlap integral indicates no hybridization between the HOMO band and $3d_{z^2}$ band, in other words, these two bands are almost independent.

IV-B-3 Metal to Insulator Transition of One-Dimensional Bis(1,2-benzoquinonedioximato)platinum(II), $\text{Pt}(\text{bqd})_2$, at Low Temperatures and High Pressures

TAKEDA, Keiki¹; SHIROTANI, Ichimin¹; SEKINE, Chihiro¹; YAKUSHI, Kyuya
(¹Muroran Inst. Tech.)

[*J. Phys. Condens. Matter* **12**, L483 (2000)]

The electrical resistivity of the high quality single crystals of one-dimensional bis(1,2-benzoquinonedioximato)platinum(II), $\text{Pt}(\text{bqd})_2$, has been studied at low temperatures and high pressures under hydrostatic conditions. The resistivity along the c -axis abruptly decreases with increasing pressure up to 0.9 GPa at room temperature. $\text{Pt}(\text{bqd})_2$ with an energy gap of about 0.3 eV at ambient pressure indicates the insulator-to-metal (IM) transition at around 0.8 GPa. The x-ray diffraction and the electronic spectrum of $\text{Pt}(\text{bqd})_2$ have been studied at room temperature and high pressures. The mechanism of the IM transition of $\text{Pt}(\text{bqd})_2$ is discussed. Below 235 K the resistivity of $\text{Pt}(\text{bqd})_2$ increases with decreasing temperature at around 0.8 GPa. The metal-to-insulator (MI) transition for $\text{Pt}(\text{bqd})_2$ is found at around 235 K under 0.8 GPa. This is the first example that the one-dimensional metal formed from single molecules shows the MI transition at low temperatures.